1   Improved Runoff Simulations for a Highly Varying Soil Depth and Complex Terrain

2   Watershed in the Loess Plateau with Community Land Model Version 5

3   Jiming Jin[1†], Lei Wang[2,3†], Jie Yang[2,3], Bingcheng Si[4], and Guoyue Niu[5,6]

4   [1]College of Resources and Environment, Yangtze University, Wuhan 430100, Hubei,

5   China

6   [2]College of Water Resources and Architectural Engineering, Northwest A & F

7   University, Yangling 712100, Shaanxi, China

8   [3]Key Laboratory of Agricultural Soil and Water Engineering in Arid and Semiarid

9   Areas, Ministry of Education, Northwest A & F University, Yangling 712100, Shaanxi,

10   China

11   [4]Department of Soil Science, University of Saskatchewan, Saskatoon, SK S7N 5A8,

12   Canada

13   [5]Biosphere 2, the University of Arizona, Tucson, AZ 85623, USA

14   [6]Department of Hydrology and Water Resources, University of Arizona, Tucson, AZ

15   85721, USA

16   Correspondence: Jiming Jin (jimingjin99@gmail.com)

17   † These authors contributed equally to this study

Abstract. This study aimed to improve runoff simulations and explore deep soil hydrological processes for a watershed in the center of the Loess Plateau (LP), China. This watershed, the Wuding River Basin (WRB), has very complex topography, with soil depths ranging from 0 to 197 m. The hydrological model used for our simulations was Community Land Model version 5 (CLM5) developed by the National Center for Atmospheric Research. Actual soil depths and river channels were incorporated into CLM5 to realistically represent the physical features of the WRB. Through sensitivity tests, CLM5 with 150 soil layers with the observed variable soil depths produced the most reasonable results and was adopted for this study. Our results showed that CLM5 with actual soil depths significantly suppressed unrealistic variations of the simulated sub-surface runoff when compared to the default simulations. In addition, when compared with the default version with 20 soil layers, CLM5 with 150 soil layers slightly improved runoff simulations, but generated simulations with much smoother vertical water flows that were consistent with the uniform distribution of soil textures in our study watershed. The runoff simulations were further improved by the addition of river channels to CLM5, where the seasonal variability of the simulated runoff was reasonably captured. Moreover, the magnitude of the simulated runoff remarkably decreased with increased soil evaporation by lowering the soil water content threshold, which triggers surface resistance. The lowered threshold was consistent with the loess soil, which has a high sand component. Such soils often generate stronger soil evaporation than soils dominated by clay. Finally, with the above changes in CLM5, the simulated total runoff matched very closely with observations. When compared with those for the default runoff simulations, the correlation coefficient, root-mean-square error, and Nash Sutcliffe coefficient for the improved simulations changed dramatically from 0.02, 10.37 mm, and -12.34 to 0.62, 1.8 mm, and 0.61. The results

43 in this study provide strong physical insight for further investigation of hydrological

44 processes in complex terrain with deep soils.

45 Key words: CLM5, complex terrain, soil depth, runoff

46

47 1 Introduction

48 Understanding runoff processes in regions with very complex topography is important

49 to managing and predicting water resources. Such an understanding can assist in

50 quantifying the allocation of water resources (Chen et al., 2013; Camacho et al., 2015),

51 evaluating surface and groundwater vulnerability to natural and anthropogenic

52 processes (Uhlenbrook et al., 2002), improving drought and flood management

53 (Camacho et al., 2015), and predicting the amount and spatiotemporal distribution of

54 water resources (Saraiva Okello et al., 2018). However, complex topography leads to

55 intricate runoff processes (Jencso et al., 2011), causing uncertain estimation of water

56 resources. Therefore, it is crucial to investigate runoff processes for the well-being of

57 topographically complex regions.

58

59 As the largest area covered by continuous loess soils in the world (Fu et al., 2017; Zhu

60 et al., 2018), the Loess Plateau (LP) in China has complicated hydrological processes

61 because of its extremely complex topography and unique soil types. Due to an arid and

62 semi-arid climate and a population of more than 100 million (Zhang et al., 2018), this

63 region experiences severe water shortages (Xiao et al., 2019). It is essential to

64 accurately estimate the spatiotemporal distribution of water resources in this region of

65 complex terrain. Soil depth in the LP can reach 350 m (Zhu et al., 2018; Li et al., 2019),

66 making it difficult to measure deep soil hydrological processes and understand runoff

67 generation (Shao et al., 2018; Liu et al., 2012). In addition, terrain in the LP includes

68 loess tablelands, ridges, hills, gullies, and river channels (Fu, 1989), all of which have

69 quite different runoff generation processes (Liu et al., 2012). In loess tablelands with

70 deep water tables (Huang et al., 2013; Shao et al., 2018), the soils store most infiltrated

71 water, generate insignificant surface runoff, and remarkably delay sub-surface runoff.

72 Areas in the LP with gullies and river channels usually have high water tables (Liu et

73 al., 2012) and can easily be saturated during precipitation events, generating a large

74 amount of surface runoff. Especially, extreme rainfall events that mostly occur over the

75 summer monsoon season (Tian et al. 2020) produce strong soil erosion and a large

76 amount of fast infiltration-excess surface runoff to the river channels in hillslope areas,

77 sometimes causing severe flooding. In the meantime, the loess soils that dominate the

78 LP have a large capillary porosity, with loose and homogeneous textures due to a high

79 sand component, often resulting in high evaporation (Li et al., 1985; Lei, 1987; Han et

80 al., 1990; Wang and Shao, 2013). A better understanding of the hydrological processes

81 within the complex terrain and special soil types of the LP is vital to improving the

82 prediction of water resources in this region.

83

84 Numerical hydrological models are essential tools to investigate runoff processes in the

85 LP. Field measurements such as those from tracer techniques (Huang et al., 2011; Li et

86 al., 2017; Huang et al., 2017; Huang et al., 2019; Xiang et al., 2019) have been made to

87 quantify the hydrological processes in the LP, but these measurements have significant

88 limitations, including short temporal and small spatial coverage, which cannot account

89 for the processes at watershed scales. Hydrological models based on mass and energy

90 equations are effective in simulating the long-term spatiotemporal variability of runoff

91 at watershed scales (Döll and Fiedler, 2007; Turkeltaub et al., 2015; Shao et al., 2018).

92 Hydrological models can also simulate the quantity of different components in the

93   water budget (e.g., surface runoff, subsurface, etc.) that are difficult or impossible to be

94   measured directly. Based on detailed soil information at a depth of 98 m at a research

95   site on the Changwu tableland in the LP, Shao et al. (2018) used a hydrological model

96   to generate reasonable simulations for deep soil percolation and groundwater level.

97   Their study provides important clues (e.g., high-resolution soil layering) for exploring

98   deep soil hydrological processes and producing reliable runoff simulations at a

99   watershed scale in the LP. Therefore, it is apparent that hydrological models can

100   overcome the drawbacks of field experiments.

101

102   However, in hydrological models, soil depth and river channels are very important in

103   simulating soil water movement and storage and runoff processes, especially in regions

104   with complex topography (Tesfa et al., 2009; Fu et al., 2011). Soil depth is set to a

105   constant in most hydrological models (Shangguan et al., 2017). For example, the Noah

106   (Ek et al., 2003) and Noah MP (Niu et al., 2011) models have a fixed soil depth of 2 m,

107   which cannot represent the realistic spatial distribution of soil depth in the LP, which

108   ranges from 0 to 350 m. In addition, soil depth in most river channels with exposed

109   bedrock in the LP is close to zero (Jing and Cheng, 1983; Li et al., 2017; Zhu et al.,

110   2018), and areas dominated by these channels are very important in generating runoff.

111   Some hydrological models such as CLM5 and the Soil and Water Assessment Tool

112   (Neitsch et al., 2011) have embedded river routing schemes. In these schemes, the river

113   channels described based on elevation differences still have the same soil depth as other

114   places without these channels, which cannot reflect the actual conditions in the LP and

115   many other regions where soil depth changes significantly across rivers. Thus, soil

116   depth variations and river channels need to be considered in hydrological models for

117   better soil water flow and runoff simulations.

118   The objective of this study was to use CLM5 to improve runoff simulations and better

119   understand the hydrological processes with varying soil depths for a very complex

120   topography watershed in the LP. To achieve this objective, the highly varying soil

121   depths and river channels were incorporated into CLM5 to realistically represent the

122   features of the watershed. In fact, Brunke et al. (2016) have conducted a study with

123   CLM version 4.5 by including varying soil depths at a global scale where the runoff

124   simulations are focused at grid cell scales, which cannot be evaluated with actual

125   streamflow data. However, evaluating hydrological simulations at watershed scales is

126   essential to improving our understanding of runoff processes. In this study, the most

127   important finding was that river channels where the soil depth is often equal or close to

128   zero played a vital role in runoff simulations especially in complex topography areas.

129   According to our extensive literature search, river channels are not configured in most

130   of existing land surface and hydrological models. In addition, although this study

131   focused on a relatively small watershed, our runoff simulation methods and science

132   ideas can be easily transferred to investigate the hydrological processes in other

133   watersheds across the world with observed soil depth and river channel information.

134   The text is laid out as follows: Sections 2 and 3 introduce the study area and data,

135   respectively, Section 4 provides the model description, Section 5 describes the

136   methodology, Section 6 includes the results, and the conclusions are in Section 7.

137

138   2 Study Area

139   The Wuding River Basin (WRB) was selected as the study area. This basin, with an

140   area of about 30,261 km^2, is in the center of the LP (Figure 1a), which is the largest

141   continuous loess area in the world (~640,000 km^2) (Fu et al., 2017; Zhu et al., 2018).

142   The WRB shows complex geomorphic characteristics including tablelands, ridges, hills,

143 gullies, and river channels (Liu et al., 2012). The main land use types in the WRB are

144 bare ground, grassland, and sparse forest. Across the basin, soil thickness generally

145 ranges from 0 to 200 m (Liu, 2016), and the loess, consisting mainly of silt and sand

146 (Li et al., 1985), is relatively homogeneous in the vertical direction (Huang et al., 2013;

147 Xiang et al., 2019). The WRB has a continental monsoon climate with mean annual

148 precipitation of around 400 mm, about 70% of which falls during the flood season from

149 June through September, based on observations over the period of 1956-2010

150 (http://data.cma.cn/). Figure 1b shows the geographic distribution of the observed soil

151 depth for the WRB, which is discussed again in Section 3.2.
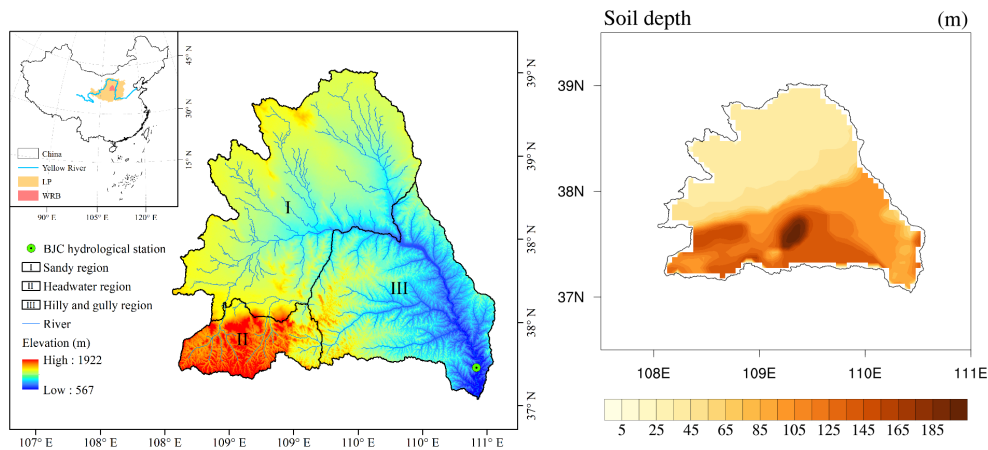
152
153 Figure 1. a) Location of the Loess Plateau (LP) and WRB in China; b) The geographic
154 distribution of the observed soil depth for the WRB.
155

156 3 Data

157 3.1 Meteorological and runoff data

158 High-quality meteorological and runoff data for the WRB were used to force and

159 evaluate CLM5, respectively. The Global Soil Wetness Project phase 3 (GSWP3)

160 meteorological dataset (http://hydro.iis.u-tokyo.ac.jp/GSWP3/index.html) was selected

161 to drive the model for this study. The GSWP3 dataset contains seven climate forcing

162 variables, including precipitation, air temperature, downward shortwave and longwave

163 radiation, specific humidity, surface pressure, and wind speed. These data cover the

164   period of 1901-2010 with a spatial resolution of 0.5 ° at a 3-hour time step. Meanwhile,

165   we obtained the observed monthly runoff data of the Baijiachuan (BJC) hydrological

166   station from the Data Sharing Network of Earth System Science

167   (http://loess.geodata.cn/index.html). The BJC station is located at the WRB outlet and

168   its drainage area covers ~98% of the basin. These runoff data were used to assess CLM5

169   output.

170

171   3.2 Soil data

172   Soil depth data for the WRB as shown in Figure 1b were obtained from different sources.

173   We first collected and recorded 61 soil depths for the WRB and nearby areas from ~15

174   published papers and books (not cited here). In addition, two soil depth maps for the

175   WRB were obtained from Qi et al. (1991) and Wang (2016) and were digitized. Soil

176   depth data for model grids with gullies and rivers were derived based on digital

177   elevation model (DEM) data. Soil depth in gullies and rivers was assumed to be 0 due

178   to the exposure of bedrock (Jing and Cheng, 1983; Li et al., 2017; Zhu et al., 2018).

179   The elevations of these gully and river channels were retrieved from a DEM at a

180   resolution of 90 m. The differences between these elevations and those at a 5 km

181   resolution were used to represent the soil depth in model grids with gullies and rivers.

182   This is different from river routing that is based only on one DEM. The proportion of

183   the total gully and river area to the entire WRB area (defined as P_{gr} hereafter) was

184   determined with the Cressman method (Cressman, 1959). A value of 0.3 is suggested

185   by Qi et al. (1991) for the LP. In this study, we identified the optimal P_{gr} value through

186   sensitivity tests by setting different interpolation radii in the Cressman method. The soil

187   depth data from these sources were then combined and interpolated into a 5 km

188   resolution, still based on the Cressman method.

189   Soil texture data for the WRB were necessary input into CLM5. These data were

190   derived from a soil type map for the LP (http://loess.geodata.cn) and included three soil

191   layers: 0-20, 20-76, and 76-180 cm. For soil layers deeper than 180 cm, the texture data

192   for the 76-180 cm layer were applied.

193

194   4 Model description

195   CLM5 was used in this study for runoff simulations. This model was developed by the

196   National Center for Atmospheric Research. The CLM5 includes one vegetation layer,

197   up to five snow layers, and 20 soil layers. In the model, each grid cell is split into

198   different land units including vegetated surface, lake, urban, glacier, and cropland. The

199   spatial distribution and seasonal climatology of the plant functional types for CLM5 are

200   derived from MODIS satellite land-surface data products (Lawrence and Chase, 2007).

201   CLM5 uses the simplified TOPMODEL (Niu et al., 2005) to parameterize runoff, which

202   is partitioned into surface and sub-surface runoff. Surface runoff is calculated based on

203   the saturation-excess mechanism. Sub-surface runoff is produced when saturated

204   conditions occur within the soil column. CLM5 is attached with a river routing module

205   for runoff simulations. However, in this study, we focused our simulations on a monthly

206   time scale at which the river flow should be able to travel from the farthest point to the

207   outlet of the WRB with an area of 30,261 km^2 that can easily fit into a 200 km by 200

208   km box. Thus, we turned off the river routing module during our simulations   and used

209   the total runoff over the entire watershed to compare with observations.

210

211   In CLM5, soil evaporation is affected by soil resistance, which is associated with a dry

212   surface layer (DSL) (Swenson and Lawrence, 2014). A DSL forms near the soil surface

213   in the model when the soil water content in the top layer is below a threshold value

214   (SWC$_{th}$), which is set to 80% of the soil porosity of the top layer (SWC$_{sat,1}$). The

215   formation of the DSL generates soil resistance, limiting soil evaporation. Meanwhile,

216   CLM5 uses Richard's equation and Darcy's law to describe changes in soil water

217   content (SWC) and soil water flux. The soil hydraulic conductivity and retention used

218   in these equations are determined by the soil texture and the SWC of the previous time

219   step, based on Clapp and Hornberger (1978), Cosby et al. (1984), and Lawrence and

220   Slater (2007).

221

222   5 Methodology

223   5.1 Soil layering

224   As mentioned, soil depth in the WRB is strongly variable, with a range of 0-200 m.

225   Although CLM5 is configured with variable soil depth, the default soil depth in CLM5

226   is set to a constant of 8.03 m (see Section 2.2.2.1 in Lawrence et al. 2018) and is

227   discretized into 20 layers defined as hydrological active layers (HALs) to distinguish

228   them from the five bedrock layers set in the model. In this study, we compared the

229   simulations with a default fixed soil depth to those with the observed variable soil

230   depths for the WRB based on the soil depth data shown in Figure 1b.. Eight sensitivity

231   tests were conducted with soil layer numbers (SLNs) of 20, 50, 75, 100, 125, 150, 175,

232   and 200 to determine the optimal soil layering method for runoff simulations in the

233   WRB (Tables 1a and 1b). In each sensitivity test, the SLN is the same for the entire

234   WRB, and the HAL number is identified based on the input soil depth for each soil

235   column. Layers that are not HALs are treated as bedrock layers and are not used in the

236   hydrology calculations in the model. These sensitivity simulations were compared to

237   those with the default options of CLM to examine how the vertical resolution with

238   observed variable soil depths affected the runoff simulations for the WRB.

Table 1a. Thickness (m) of each soil layer for different SLNs (20, 50, 75, and 100)

Sequence	SLN				Sequence	SLN			
	20	50	75	100		20	50	75	100
1	0.02	0.02	0.02	0.02	18-20	40.00	2.00	1.00	0.64
2	0.04	0.04	0.04	0.04	21-25		4.00	1.00	0.84
3	0.06	0.06	0.06	0.06	26-35		4.00	2.00	1.04
4	0.08	0.08	0.08	0.08	36-40		6.00	2.00	1.04
5	0.12	0.12	0.12	0.12	41-45		8.00	2.50	1.44
6	0.16	0.16	0.16	0.16	46-50		10.00	3.00	1.44
7	0.20	0.20	0.20	0.20	51-55			3.00	1.44
8	0.24	0.24	0.24	0.24	56-65			4.00	2.00
9	0.28	0.28	0.28	0.28	66			5.14	2.40
10	0.32	0.32	0.32	0.32	67-70			6.00	2.40
11	0.64	0.64	0.64	0.64	71-75			8.00	2.40
12	2.00	1.00	0.80	0.64	76-85				2.80
13	4.84	1.00	0.80	0.64	86-89				4.00
14	12.00	1.04	0.80	0.64	90				4.68
15	16.00	1.80	0.80	0.64	91-95				5.00
16-17	20.00	2.00	1.00	0.64	96-100				6.00

Table 1b. Thickness (m) of each soil layer for different SLNs (125, 150, 175, and 200)

Sequence	SLN				Sequence	SLN			
	125	150	175	200		125	150	175	200
1	0.02	0.02	0.02	0.02	51-70	1.14	1.14	1.14	1.04
2	0.04	0.04	0.04	0.04	71	1.58	1.40	1.20	1.04
3	0.06	0.06	0.06	0.06	72-79	2.00	1.40	1.20	1.04
4	0.08	0.08	0.08	0.08	80-85	2.00	1.50	1.20	1.04
5	0.12	0.12	0.12	0.12	86-100	2.40	1.60	1.20	1.04
6	0.16	0.16	0.16	0.16	101	2.40	1.60	1.20	1.02
7	0.20	0.20	0.20	0.20	102-104	2.40	1.60	1.20	1.14
8	0.24	0.24	0.24	0.24	105	2.40	1.60	1.28	1.14
9	0.28	0.28	0.28	0.28	106-120	2.80	1.80	1.30	1.14
10	0.32	0.32	0.32	0.32	121-125	4.00	1.80	1.30	1.14
11-25	0.64	0.64	0.64	0.64	126-130		2.00	1.30	1.14
26-30	0.84	0.84	0.84	0.64	131-150		2.00	1.40	1.14
31-40	0.84	0.84	0.84	0.84	151-155			1.40	1.14
41	1.04	1.02	1.04	0.84	156-175			1.50	1.14
42-45	1.04	1.04	1.04	0.84	176-200				1.14
46-50	1.14	1.14	1.14	0.84					

5.2 Model spin-up and simulations

All runs in this study needed model spin-up to ensure that the soil moisture of each

HAL reached equilibrium. We found that the spin-up period could last for 50-400 years

247 for different initial SWC conditions and soil depths in the WRB. When the initial SWC

248 was set to 0.2 mm^3/mm^3 with observed soil depths, the spin-up period was about 50

249 years, which was adopted for production simulations in this study. We performed two

250 cycles of continuous simulations for 1901-2010. The first cycle was discarded for spin-

251 up, and the second cycle was retained for analysis. In this study, each sensitivity run

252 had its own spin-up.

253

254 6 Results and Analysis

255 6.1 Default runoff simulation

256 We conducted a default run to evaluate the performance of the original CLM5 in

257 simulating runoff in the WRB. The model remarkably overestimated monthly total and

258 sub-surface runoff when compared with observations from the BJC hydrological station

259 over 1956-1969, a period with minimal human activity (Jiao et al., 2017). The

260 correlation coefficient (R^2), root mean square error (RMSE), and Nash Sutcliffe

261 efficiency (NSE) were 0.02, 10.37 mm, and -12.34, respectively. We can see that the

262 overestimation was due mainly to the unrealistic simulations of sub-surface runoff. The

263 reasons for these erroneous simulations are discussed in detail in the following sections.
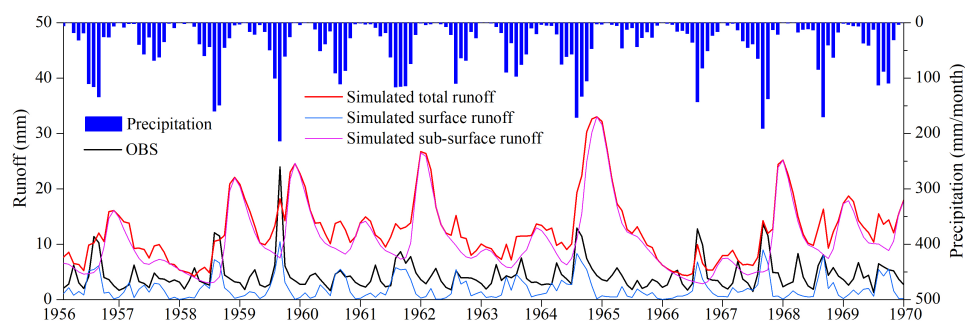
264
265 Figure 2. Observed monthly precipitation and runoff (black line) and simulated total
266 runoff, surface runoff, and sub-surface runoff in the default run from 1956 to 1969. The
267 observed monthly precipitation is for the entire WRB, and the OBS and simulations are
268 for the BJC hydrological station.

269

270

271 6.2 Effects of soil depth on runoff simulations

272 We examined how the simulated runoff for the WRB was affected by the actual soil

273 depths (40-197 m) that were inputted into CLM5 with a default SLN of 20. As shown

274 in Figure 3, CLM5 with deep soils greatly suppressed the seasonal variability of sub-

275 surface runoff and reduced the magnitude of surface runoff when compared with the

276 CLM5 simulations with a uniform soil depth of 8 m. The R^2, RMSE, and NSE between

277 observations and the simulations with actual soil depths were 0.04, 9.8 mm, and -10.96,

278 respectively. Although the actual soil depth data for the WRB were included in CLM5,

279 the runoff simulations were still remarkably different from observations in both

280 variability and magnitude. Hence, the runoff simulations for the WRB need to be further

281 explored and understood.
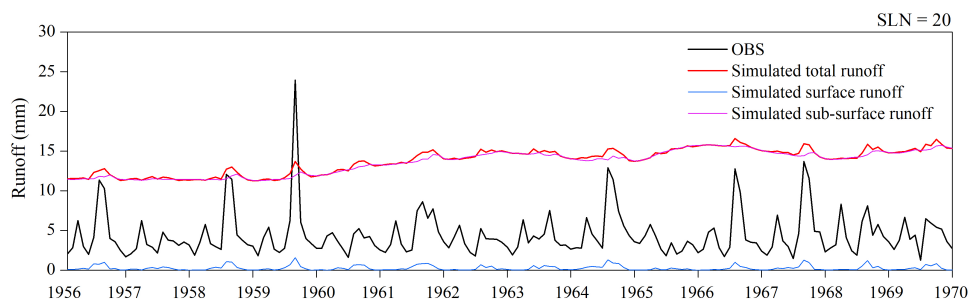
282
283 Figure 3. Observed and simulated total runoff, surface runoff, and sub-surface runoff
284 from 1956 to 1969 by the run with actual soil depths. The SLN was set to 20.

285

286 6.3 Effects of soil layering on runoff simulations

287 The eight soil layering methods mentioned in Section 3.2 were applied to CLM5 with

288 the actual soil depths for the WRB to investigate the effects of soil layering on the

289 runoff simulations. We can see that all the CLM5 runs generated similar temporal

290 patterns of simulated total runoff, as shown in Figure 4a. Obviously, the soil layering

291 methods had almost no effect on the surface runoff simulations (Figure 4b), while these

292 methods did affect the sub-surface runoff simulations to some extent (Figure 4c). When

293 the vertical spatial resolution increased from 20 to 200 soil layers, the RMSE of the

simulated total runoff decreased until the SLN was equal to 75, and then the errors

reached a minimum for SLN ranging from 100 to 200 (Figure 4d). Although the model

with 75 soil layers seemed to be an efficient case, the soil layering method was further

examined with vertical soil moisture profile simulations.
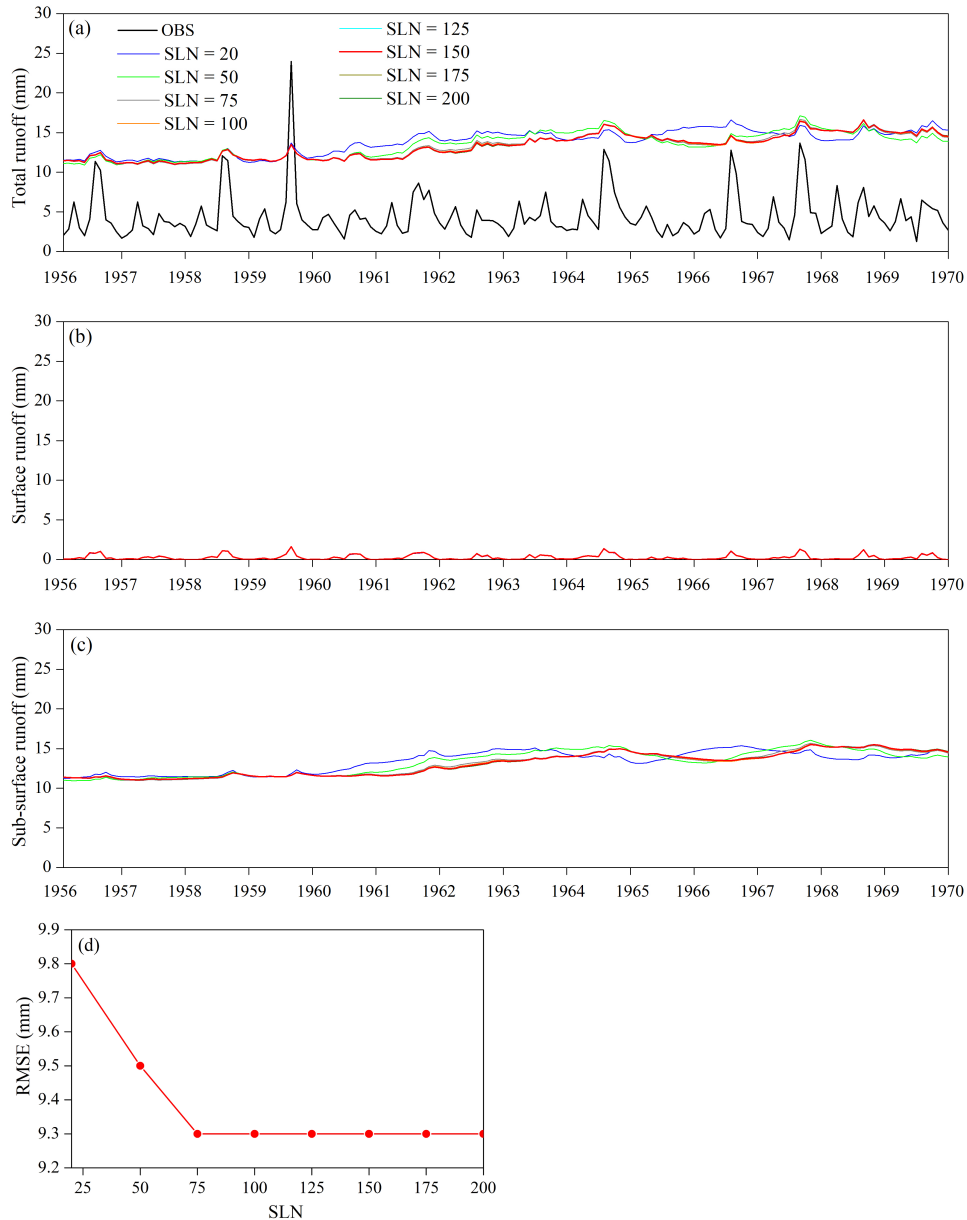
Figure 4. (a) Observed and simulated monthly runoff for the BJC hydrological station;
(b) simulated surface runoff; (c) simulated sub-surface runoff; (d) RMSEs of the
simulated total runoff. All simulations were produced with different SLN values.

We selected a point (37.53 °N, 109.33 °E) with the deepest soil depth of 197 m in the

WRB to study the soil layering method based on vertical soil moisture profile

308 simulations. As shown in Figure 5, the coarser-resolution simulations (SLN ≤ 125)

309 resulted in alternating persistent wet-dry layers throughout our study period, and this

310 alternation gradually weakened with increasing SLN. When the SLN was equal to 150,

311 the wet-dry alternation almost disappeared. We examined the model numerical method

312 and found that the coarser resolution numerically caused smaller soil matric potential

313 (SMP) gradients between the soil layers, leading to the wet-dry alternation. These

314 vertical soil moisture simulations indicated that CLM5 could produce smooth soil water

315 flow simulations with at least 150 soil layers at a soil depth of 197 m to avoid these

316 numerical issues, although the RMSE of the simulated total runoff reached the

317 minimum value with SLN equal to 75. Therefore, in the following simulations, we set

318 the model soil layers to 150. With this soil layering, the R^2, RMSE, and NSE for the

319 total runoff simulations were 0.07, 9.3 mm, and -9.71, respectively.
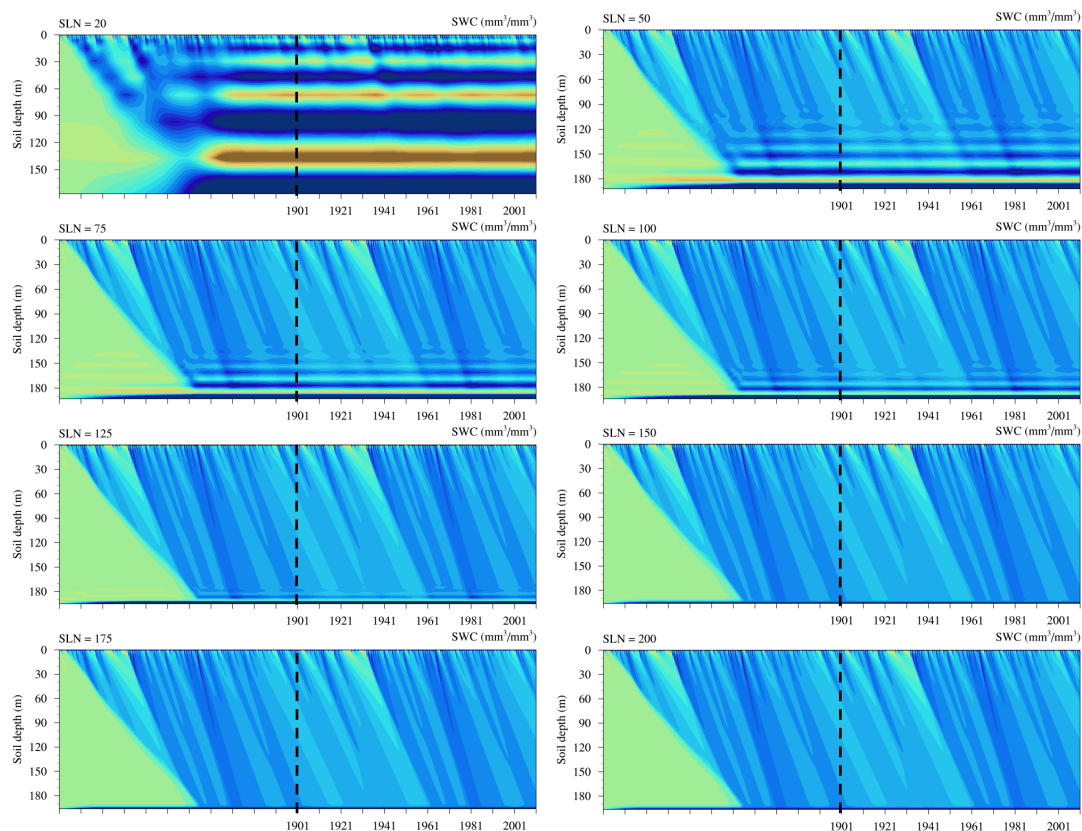
320
321
322
323
324 Figure 5. Simulated vertical monthly SWC profiles for the selected point in the WRB
325 during both the spin-up (left of the black dashed line) and simulation (right of the black
326 dashed line) periods. All simulations were conducted with different SLN values.
327

328 6.4 Effects of P_{gr} on runoff simulations

329 In addition to the actual soil depth and high-resolution soil layering, we prescribed the

330 river channels for the WRB in CLM5 to explore the effects of those channels on runoff

331 simulations. Figure 6 shows the spatial distribution of the river channels for the WRB

332 with different values of P_{gr}, a proportion of the total river channel area to the entire

333 WRB area, as previously defined. The larger the P_{gr}, the denser the river channels. Our

334 results showed that CLM5 dramatically improved the simulations of the seasonal

335 variability of total runoff (Figure 7a), and the R^2 increased to 0.41-0.56 from 0.07 for

336 the previous simulations. These improvements resulted mainly from the surface runoff

337 simulations with a much higher seasonal variability (Figure 7b). The sub-surface runoff

338 simulations did not show significant changes with the addition of the river channels to

339 CLM5 (Figure 7c). We can see that CLM5 with P_{gr} equal to 0.15 produced the lowest

340 RMSE (9.3 mm) and the highest NSE (-9.78), although the R^2 was not the highest (0.52)

341 with this P_{gr} value. Moreover, we found that the seasonal peak values of the simulated

342 surface runoff with P_{gr} values of 0.22 and 0.26 were higher than the observed peak

343 values (Figure not shown), which was not realistic. Thus, we selected 0.15 for P_{gr} for

344 the rest of our simulations.
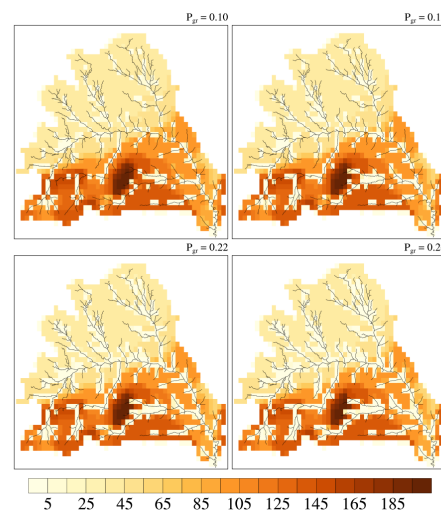
345
346 Figure 6. Spatial distributions of river channels (black lines) and soil depths for the
347 WRB with different values of P_{gr}.

348

349

350
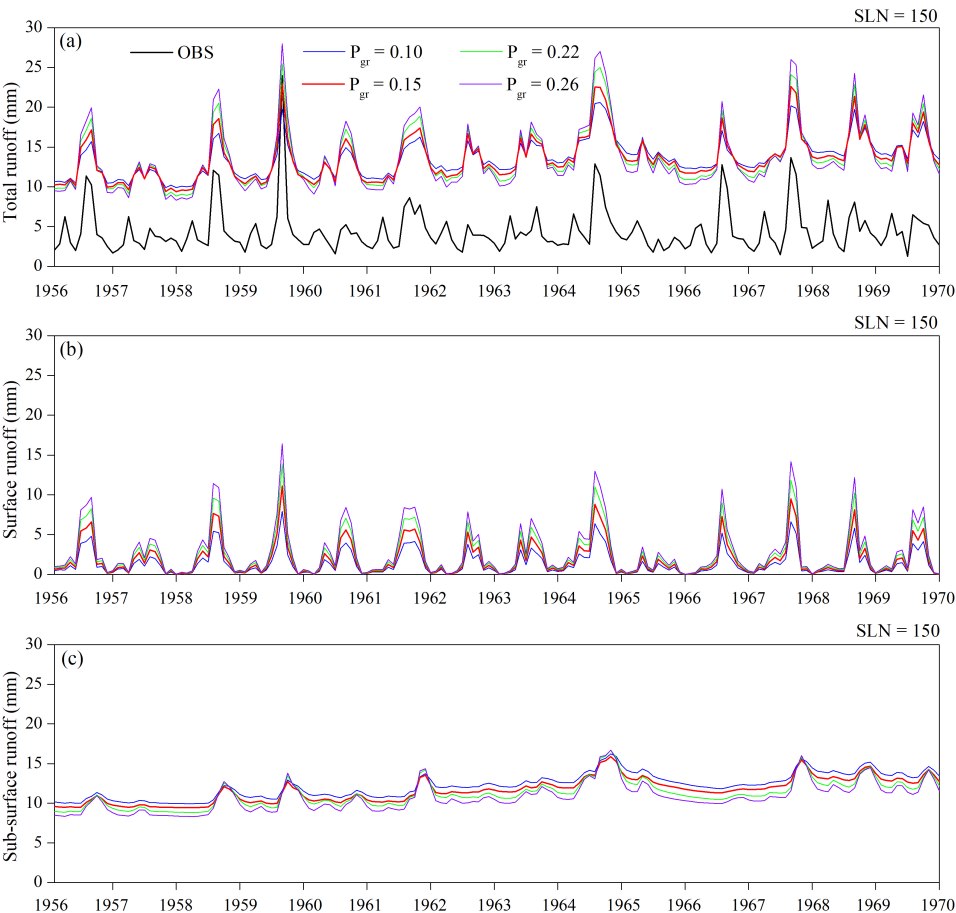
351
352 Figure 7. (a) Observed and simulated monthly runoff for the BJC hydrological station;
353 (b) simulated surface runoff; (c) simulated sub-surface runoff. All simulations were
354 produced with different P_{gr} values.

355

356 Table 2. R^2, RMSE, and NSE for total runoff simulations with different P_{gr} values

P_{gr}	0.10	0.15	0.22	0.26
R^2	0.41	0.52	0.54	0.56
RMSE (mm)	9.4	9.3	9.4	9.5
NSE	-9.90	-9.78	-10.06	-10.23

357

358 6.5 Water balance analysis

359 We looked into the water balance for the WRB and attempted to further reduce the

360 biases of the runoff simulations. In the previous sections, the more realistic conditions

361 of the WRB (actual soil depths, high-resolution soil layering, and river channels) were

362 incorporated into CLM5 to improve the runoff simulations, but the simulations were

363 still far away from observations. Tian et al. (2018) indicated that the change in water

storage in the WRB approached zero over a period of 13 years. Our study focused on a period of 14 years (1956-1969). Thus, we estimated the mean evapotranspiration (ET) with observed precipitation and runoff over our study period by assuming a water storage change of zero in the WRB as follows:

$$ET_{avg} = P_{avg} - R_{avg} \tag{1}$$

where ET_{avg}, P_{avg}, and R_{avg} are mean ET (mm), precipitation (mm), and runoff (mm) over 1956-1969, respectively. Here, P_{avg} is 454.7 mm, R_{avg} is 53.2 mm, and the estimated ET_{avg} is 401.5 mm. However, the simulated mean ET over the study period was 267.8 mm, which was far below the estimated value. According to the soil evaporation parameterization in CLM5, when the SWC of the top soil layer (SWC_1) was less than SWC_{th}, a DSL formed to resist soil evaporation. In CLM5, the SWC_{th} is defined as 80% of $SWC_{sat,1}$. However, previous studies (Lee and Pielke, 1992; Sakaguchi and Zeng, 2009; Flammini et al., 2018) found that soil evaporation starts to decrease significantly when the surface SWC is less than the field capacity. Yang et al. (1985) also found that soil evaporation in the LP slows down when the surface SWC becomes lower than a stable capacity that is close to the field capacity. Thus, in this study, we changed the SWC_{th} to the $SWC_{fc,1}$ to conduct one additional simulation. With this modification, the simulated annual ET fluctuated around the estimated mean ET for our study period (401.5 mm), and the simulated 14-year mean value was 392.5 mm, which was close to the estimated mean. Very importantly, the simulated total runoff drastically reduced to match observations by increasing ET (Figure 8). When compared with those for the simulations in the last section, R^2 increased from 0.52 to 0.62, RMSE decreased from 9.3 to 1.8 mm, and NSE increased dramatically from -9.78 to 0.61. Therefore, we remarkably improved runoff simulations with more accurate ET simulations in addition to the more realistic WRB features.
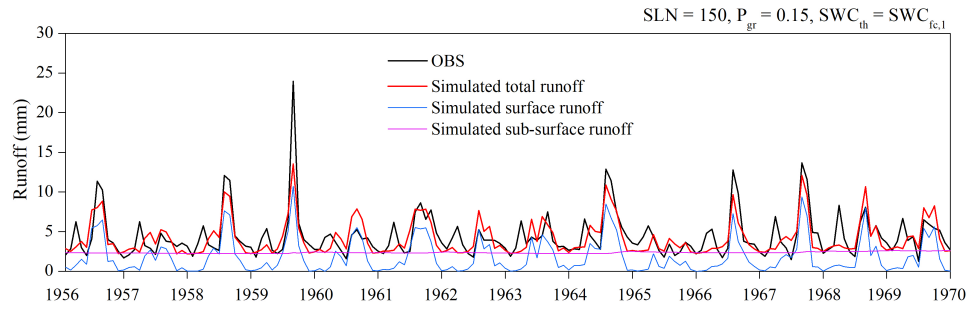
Figure 8. Time series of observed monthly runoff (black line) for the BJC hydrological station and simulated monthly total (red line), surface (blue line), and sub-surface runoff (pink line).

7 Conclusions and discussion

This study was intended to improve runoff simulations with CLM5 for the complex topography of the WRB and to improve our understanding of deep soil hydrological processes. In CLM5, we included actual soil depths for the WRB ranging from 0 to 197 m and added the river channels for this watershed. We tested eight soil layering methods and found that CLM5 with at least 150 soil layers could produce rational simulations for both runoff and the vertical soil moisture profile. Different values of river channel density were examined with CLM5, showing that a ratio of 15% of the total river channel area to the entire WRB area generated the most reasonable results.

With the above model settings, our simulations showed that CLM5 with actual soil depths greatly suppressed the seasonal variability of simulated sub-surface runoff and reduced the simulated surface runoff when compared with the default simulations with a uniform soil depth of 8 m. In addition, CLM5 with finer-resolution soil layering (SLN ≥ 150) led to more accurate runoff and smoother vertical soil water flow simulations than that with coarser-resolution layering, and the latter was consistent with the homogeneous distribution of vertical soil texture in the WRB. The addition of river channels for the WRB to CLM5 significantly increased the seasonal variability of simulated surface runoff, remarkably improving the seasonal variability of simulated

total runoff. Moreover, more accurate simulations of soil evaporation in the WRB dramatically reduced the simulated sub-surface runoff and improved the total runoff simulations.

Limitations still exist in this study. We used atmospheric forcing data at a 5 km resolution to drive CLM5, but for our study region with very complex terrain, this resolution may not be sufficient and could potentially have generated errors in our simulations. In the meantime, it is very important to expand this study to a larger or even global scale, and accurate soil depth and detailed soil texture data would be vital to such an expanded study. In addition, soil hydraulic properties may change with depth, but this study did not consider such changes, and this needs to be tested in future studies. Despite these limitations, it is clear that our final runoff simulations with an improved CLM5 were highly accurate, and our understanding of deep soil hydrological processes has advanced.

Author contributions. JJ and LW designed the research; LW conducted the simulations; LW and JY collected the soil depth data; JJ and LW analyzed the data; JY was involved in several sensitivity simulation tests; JJ and LW wrote the paper; BS and GN edited the paper and provided substantial comments for scientific clarification.

Code and data availability. Our improved model and data are available at https://doi.org/10.5281/zenodo.5044541.

Competing interests. The authors declare that they have no conflict of interest.

Acknowledgments. This research was funded by the National Natural Science Foundation of China (No. 41571030, No. 91637209, and No. 91737306).

References

Camacho, V. V., Saraiva Okello, A. M. L., Wenninger, J. W., and Uhlenbrook, S.: Understanding runoff processes in a semi-arid environment through isotope and hydrochemical hydrograph separations, Hydrol. Earth Syst. Sci. Discuss., 19, 4183-4199, https://doi.org/10.5194/hessd-12-975-2015, 2015.

Chen, L., Sela, S., Svoray, T., and Assouline, S.: The role of soil-surface sealing, microtopography, and vegetation patches in rainfall-runoff processes in semiarid areas, Water Resour. Res., 49, 5585-5599, 2013.

Clapp, R. B. and Hornberger, G. M.: Empirical equations for some soil hydraulic properties, Water Resour. Res., 14, 601-604, 1978.

Cosby, B. J., Hornberger, G. M., Clapp, R. B., and Ginn, T. R.: A statistical exploration of the relationships of soil moisture characteristics to the physical properties of soils, Water Resour. Res., 20, 682-690, 1984.

Cressman, G. P.: An operational objective analysis system, Mon. Weather Rev., 87, 367-374, 1959.

Döll, P. and Fiedler, K.: Global-scale modeling of groundwater recharge, Hydrol. Earth Syst. Sci. Discuss., 12, 863-885, https://doi.org/10.5194/hess-12-863-2008, 2008.

Ek, M. B., Mitchell, K. E., Lin, Y., Rogers, E., Grunmann, P., Koren, V., Gayno, G., and Tarpley, J., D.: Implementation of Noah land surface model advances in the National Centers for Environmental Prediction operational mesoscale Eta model, J. Geophys. Res., 108, 8851, https://doi.org/10.1029/2002JD003296, 2003.

Flammini, A., Corradini, C., Morbidelli, R., Saltalippi, C., Picciafuoco, T., and Giráldez, J. V.: Experimental analyses of the evaporation dynamics in bare soils under natural conditions, Water Resour. Manag., 32, 1153-1166, https://doi.org/10.1007/s11269-017-1860-x, 2018.

Fu, B.: Soil erosion and its control in the Loess Plateau of China, Soil Use Manage., 5, 76-82, 1989.

Fu, B., Wang, S., Liu, Y., Liu, J., Liang, W., and Miao, C.: Hydrogeomorphic Ecosystem Responses to Natural and Anthropogenic Changes in the Loess Plateau of China, Annu. Rev. Earth Planet. Sci., 45, 223-243, https://doi.org/10.1146/annurev-earth-063016-02055, 2017.

Fu, Z., Li, Z., Cai, C., Shi, Z., Xu, Q., and Wang, X.: Soil thickness effect on hydrological and erosion characteristics under sloping lands: A hydropedological perspective, Geoderma, 167-168, 41-53, https://doi.org/10.1016/j.geoderma.2011.08.013, 2011.

Han, S., Li, Y., Shi, Y., Yang, X., Zhang, X., and Shi, Z.: The characteristic of soil moisture resources on the Loess Plateau, Bulletin of Soil and Water Conservation, 10, 36-43, 1990.

Huang, T. and Pang, Z.: Estimating groundwater recharge following land-use change using chloride mass balance of soil profiles: A case study at Guyuan and Xifeng in the Loess Plateau of China, Hydrogeology J., 19, 177-186, https://doi.org/10.1007/s10040-010-0643-8, 2011.

Huang, T., Pang, Z., and Edmunds, W. M.: Soil profile evolution following land-use change: Implications for groundwater quantity and quality, Hydrol. Process., 27, 1238-1252, https://doi.org/10.1002/hyp.9302, 2013.

Huang, T., Pang, Z., Liu, J., Yin, L., and Edmunds, W. M.: Groundwater recharge in an arid grassland as indicated by soil chloride profile and multiple tracers, Hydrol. Process., 31, 1047-1057, https://doi.org/10.1002/hyp.11089, 2017.

Huang, Y., Evaristo, J., and Li, Z.: Multiple tracers reveal different groundwater recharge mechanisms in deep loess deposits, Geoderma, 353, 204-212, https://doi.org/10.1016/j.geoderma.2019.06.041, 2019.

Jencso, K. G. and Mcglynn, B. L.: Hierarchical controls on runoff generation: Topographically driven hydrologic connectivity, geology, and vegetation, Water Resour. Res., 47, W11527, 2011.

Jiao, Y., Lei, H., Yang, D., Huang, M., Liu, D., and Yuan, X.: Impact of vegetation dynamics on hydrological processes in a semi-arid basin by using a land surface-hydrology coupled model, J. Hydrol., 551, 116-131, https://doi.org/10.1016/j.jhydrol.2017.05.060, 2017.

Jing, K. and Cheng, Y.: Preliminary study of the erosion environment and rates on the Loess Plateau, Geogr. Res., 2, 1-11, 1983.

Lawrence, D., Fisher, R., Koven, C., Oleson, K., Swenson, S., Vertenstein, M., Andre, B., Bonan, G., Ghimire, B., Kampenhout, L. V., Kennedy, D., Kluzek, E., Knox, R., Lawrence, P., Li, F., Li, H., Lombardozzi, D., Lu, Y., Perket, J., Riley, W., Sacks, W., Shi, M., Wieder, W., Xu, C., Ali, A., Badger, A., Bisht, G., Broxton, P., Brunke, M., Buzan, J., Clark, M., Craig, T., Dahlin, K., Drewniak, B., Emmons, L., Fisher, J., Flanner, M., Gentine, P., Lenaerts, J., Levis, S., Leung, L. R., Lipscomb, W., Pelletier, J., Ricciuto, D. M., Sanderson, B., Shuman, J., Slater, A., Subin, Z., Tang, J., Tawfik, A., Thomas, Q., Tilmes, S., Vitt, F., and Zeng, X.: Technical Description of version 5.0 of the Community Land Model (CLM5), National Center for Atmospheric Research, Boulder, Colorado, 2018.

Lawrence, D. M. and Slater, A. G.: Incorporating organic soil into a global climate model, Clim. Dynam., 30, 145-160, https://doi.org/10.1007/s00382-007-0278-1, 2008.

Lawrence, P. J. and Chase, T. N.: Representing a new MODIS consistent land surface in the Community Land Model (CLM5 3.0), J. Geophys. Res., 112, G01023, 2007.

Lee, T. J. and Pielke, R. A.: Estimating the soil surface specific humidity, J. Appl. Meteorol., 31, 480-484, 1992.

Lei, X.: Pore types and collapsibility of the loess in China, Science China Press, 1203-1208, 1987.

Li, Y., Han, S. and Wang, Z.: Soil water properties and its zonation in the Loess Plateau. Res. Soil Water Conserv., 1-17, 1985.

Li, Z., Chen, X., Liu, W., and Si, B.: Determination of groundwater recharge mechanism in the deep loessial unsaturated zone by environmental tracers, Sci Total Environ, 586, 827-835, https://doi.org/10.1016/j.scitotenv.2017.02.061, 2017.

Li, Z., Jasechko, S., and Si, B.: Uncertainties in tritium mass balance models for groundwater recharge estimation, J. Hydrol., 571, 150-158, https://doi.org/10.1016/j.jhydrol.2019.01.030, 2019.

Liu, D., Tian, F., Hu, H., and Hu, H.: The role of run-on for overland flow and the characteristics of runoff generation in the Loess Plateau, China, Hydrol. Sci. J., 57, 1107-1117, 2012.

Liu, Z.: The Study on the Classification of Loess Landscape and the Characteristics of Loess Stratum, M.S. thesis, College of Geological Engineering and Geomatics, Chang'an University, China, 2016.

Neitsch, S. L., Arnold, J. G., Kiniry, J. R., and Williams, J. R.: Soil and Water Assessment Tool Theoretical Documentation Version 2009. Texas Water Resources Institute Technical Report, Texas, 2011.

Niu, G. Y., Yang, Z. L., Dickinson, R. E., and Gulden, L. E.: A simple TOPMODEL-based runoff parameterization (SIMTOP) for use in global climate models, J. Geophys. Res., 110, D21106, 2005.

Niu, G., Yang, Z., Mitchell, K. E., Chen, F., Ek, M. B., Barlage, M., Kumar, A., Manning, K., Niyogi, D., Rosero, E., Tewari, M., and Xia, Y.: The community Noah land surface model with multiparameterization options (Noah-MP): 1. Model description and evaluation with local-scale measurements, J. Geophys. Res., 116, D12109, https://doi.org/10.1029/2010JD015139, 2011.

Qi, C., Gan, Z., Xi, Z., Wu, C., Sun, H., Chen, W., Liu, T., and Zhao, G.: The research of the relations between erosion landforms and soil erosion of the Loess Plateau, Shaanxi People's Education Publishing House, Shaanxi, China, 1991.

Sakaguchi, K. and Zeng, X.: Effects of soil wetness, plant litter, and under-canopy atmospheric stability on ground evaporation in the Community Land Model (CLM53. 5), J. Geophys. Res., 114, 2009.

Saraiva Okello, A. M. L., Uhlenbrook, S., Jewitt, G. P. W., Masih, I., Riddell, E. S., and Van der Zaag, P.: Hydrograph separation using tracers and digital filters to quantify runoff components in a semi-arid mesoscale catchment, Hydrol. Process., 32, 1334-1350, https://doi.org/10.1002/hyp.11491, 2018.

Shangguan, W., Hengl, T., Mendes de Jesus, J., Yuan, H., and Dai, Y.: Mapping the global depth to bedrock for land surface modeling, J. Adv. Model. Earth Syst., 9, 65-88, https://doi.org/0.1002/2016MS000686, 2017.

Shao, J., Si, B., and Jin, J.: Extreme precipitation years and their occurrence frequency regulate long-term groundwater recharge and transit time, Vadose Zone J., 17, 1-9, https://doi.org/10.2136/vzj2018.04.0093, 2018.

Swenson, S. C. and Lawrence, D. M.: Assessing a dry surface layer-based soil resistance parameterization for the Community Land Model using GRACE and FLUXNET-MTE data, J. Geophys. Res. Atmos., 119, 10,299-10,312, 2014.

Tesfa, T. K., Tarboton, D. G., Chandler, D. G., and McNamara, J. P.: Modeling soil depth from topographic and land cover attributes, Water Resour. Res., 45, W10438, 2009.

Tian, L., Jin, J., Wu, P., and Niu, G.: Assessment of the effects of climate change on evapotranspiration with an improved elasticity method in a nonhumid area, Sustainability, 10, 4589, https://doi.org/10.3390/su10124589, 2018.

Tian, L., Jin, J., Wu, P., Niu, G.-Y., and Zhao, C.: High-resolution simulations of mean and extreme precipitation with WRF for the soil-erosive Loess Plateau. Clim. Dynam., 54. 10.1007/s00382-020-05178-6, 2020.

Turkeltaub, T., Kurtzman, D., Bel, G., and Dahan, O.: Examination of groundwater recharge with a calibrated/validated flow model of the deep vadose zone, J. Hydrol., 522, 618-627, https://doi.org/10.1016/j.jhydrol.2015.01.026, 2015.

Uhlenbrook, S., Frey, M., Leibundgut, C., and Maloszewski, P.: Hydrograph separations in a mesoscale mountainous basin at event and seasonal timescales, Water Resour. Res., 38, 1096, 2002.

Wang, S.: Study on geological engineering of loess in North Shaanxi, M. S. thesis, College of Geological Engineering and Geomatics, Chang'an University, China, 2016.

Wang, Y. and Shao, M.: Spatial variability of soil physical properties in a region of the Loess Plateau of pr China subject to wind and water erosion, Land Degrad. Dev., 24, 296-304, https://doi.org/10.1002/ldr.1128, 2013.

Xiang, W., Si, B., Biswas, A., and Li, Z.: Quantifying dual recharge mechanisms in deep unsaturated zone of Chinese Loess Plateau using stable isotopes, Geoderma, 337, 773-781, https://doi.org/10.1016/j.geoderma.2018.10.006, 2019.

Xiao, J., Wang, L., Deng, L., and Jin, Z.: Characteristics, sources, water quality and health risk assessment of trace elements in river water and well water in the Chinese Loess Plateau, Sci. Total Environ., 650, 2004-2012, https://doi.org/10.1016/j.scitotenv.2018.09.322, 2019.

Yang, W., Shi, Y., and Fei, W.: Water evaporation from soils under unsaturated condition and evaluation for drought resistance of soils on Loessal Plateau, Acta Pedologica Sinica, 22, 13-23, 1985.

Zhang, F., Zhang, W., Qi, J., and Li, F.: A regional evaluation of plastic film mulching for improving crop yields on the Loess Plateau of China, Agric. For. Meteorol., 248, 458-468, https://doi.org/10.1016/j.agrformet.2017.10.030, 2018.

Zhu, Y., Jia, X., and Shao, M.: Loess thickness variations across the Loess Plateau of China, Surv. Geophys., 39, 715-727, https://doi.org/10.1007/s10712-018-9462-6, 2018.